

Tiling with triangles: parquet and $GW\gamma$ methods unified

Friedrich Krien,¹ Anna Kauch,¹ and Karsten Held¹

¹*Institute for Solid State Physics, TU Wien, 1040 Vienna, Austria*

The parquet formalism and Hedin’s $GW\gamma$ approach are unified into a single theory of vertex corrections, corresponding to a bosonization of the parquet equations. The method has no drawbacks compared to previous parquet solvers but has the significant advantage that the vertex functions decay quickly with frequencies and with respect to distances in the real space. These properties coincide with the respective separation of the length and energy scales of the two-particle correlations into long/short-ranged and high/low-energetic.

I. INTRODUCTION

The systematic calculation of vertex corrections in electronic systems historically builds upon two distinct formalisms, the parquet formalism of De Dominicis and Martin [1, 2] and the $GW\gamma$ method introduced by Hedin [3]. Although both approaches are in widespread use since the 1960’s, they have largely remained separate entities.

The parquet approach [4–10] classifies vertex corrections into three scattering channels, allowing an unbiased competition between the bosonic fluctuations in these channels [11–15]. The Hedin equations, on the other hand, aim at the particle-hole channel, with vertex corrections γ in this channel being calculated self-consistently from the derivative of the self-energy with respect to the Green’s function $\delta\Sigma/\delta G$ [16, 17]. Both formalisms constitute an exact quantum field theoretical framework, but in practice one relies on approximations: In case of the parquet formalism, the fully irreducible vertex Λ is approximated, e.g., by $\Lambda = U$ (the bare interaction) in the parquet approximation [4] or by $\Lambda = \text{local}$ in the dynamical vertex approximation [18–20]. In case of the Hedin approach, γ is approximated, e.g., by $\gamma = 1$ in the GW approximation or by simple approximations in so-called $GW\gamma$ approaches, even allowing for realistic materials calculations [16, 17, 21–26].

One difference is that the parquet formalism is formulated in terms of four-point electron-electron vertices (Feynman diagrammatic “squares”, capitalized symbols in our notation), whereas Hedin [3] formulated his equations in terms of three-point electron-boson vertices (“triangles”, lowercase symbols). The latter can be reformulated easily in terms of four-point squares, see e.g. [17], but to the best of our knowledge the parquet approach evaded hitherto a three-point (triangle) reformulation.

A second major difference between the two approaches is that the parquet equations naturally obey the crossing symmetry but typical approximations violate conservation laws [4, 20, 27–32], whereas $GW\gamma$ approximations conversely often obey conservation laws [33] but violate the crossing symmetry, and thereby the Pauli principle. Indeed, only the exact solution satisfies the crossing symmetry and the Ward identity at the same time, see Ref. [31] for a formal proof.

Aspects of both concepts come into play in the the-

ory of collective bosonic fluctuations in fermionic systems, see, for example, Ref. [34], in particular of those in superconductors [35], where the three-legged fermion-boson coupling and the screened interaction are used to construct four-point vertex corrections. However, these considerations are almost always of a phenomenological kind and only a few Feynman diagrams of interest are calculated, such as the Aslamazov-Larkin vertex correction [36, 37] (see diagram (b) in Fig. 3 below). But in terms of an overarching theory the relation between the parquet and Hedin formalisms remains, even after more than 50 years, only a tentative one.

In this paper, both approaches and viewpoints are merged into a single theory. It is shown that the parquet decomposition of the vertex function, which relies on the reducibility with respect to Green’s functions [6], can be combined with the recently introduced *single-boson exchange (SBE)* decomposition [38] that is based on the idea of reducibility with respect to the interaction, which generalizes the Hedin equations. In particular, the diagrams that are reducible with respect to the interaction can be removed exactly from the parquet expressions and suitable ladder equations can be defined which replace the Bethe-Salpeter equations. Through this reformulation we tile our diagrammatic “floor” not with conventional four-leg parquet “squares” but with three-leg “triangles”, with the exception being an irreducible “square” $\tilde{\Lambda} = \Lambda - U$, which vanishes in the parquet approximation.

The present paper is in close conjunction with Ref. [39] where the parquet equations for dual fermions [40] have been reformulated. Instead, here we show how the standard parquet approach [4–10] can be rewritten and connected with the Hedin equations [41]. An efficient real fermion parquet solver for a quantum impurity model is presented and made available [42]. Similar as for dual fermions [39], this reformulation leads to a substantially improved feasibility of the parquet solution because it removes simultaneously the high-frequency asymptotics [43] and the long-ranged fluctuations [20] from the parquet equations.

The paper is organized as follows. The Hedin and parquet formalisms are recollected in Sections II and III, respectively. The two concepts are connected and merged in Section IV. A calculation scheme is presented in Section V; and Section VI presents the implementation for a quantum impurity model and examples for the lattice

Hubbard model from the parquet approximation. Finally, Section VII summarizes our results.

II. HEDIN'S FORMALISM

In Hedin's theory the self-energy of the electronic system is expressed in terms of the Green's function G , the screened interaction W , and the vertex γ . For a single-band Hubbard-type system with the interaction $Un_{\uparrow}n_{\downarrow}$ the self-energy can be expressed in the paramagnetic case as follows [44]:

$$\Sigma_k = \frac{U\langle n \rangle}{2} - \frac{1}{2} \sum_q G_{k+q} \left[W_q^{\text{ch}} \gamma_{kq}^{\text{ch}} + W_q^{\text{sp}} \gamma_{kq}^{\text{sp}} \right]. \quad (1)$$

Here, ch and sp denote the charge and spin (or density and magnetic) combinations of the spin indices, respectively, see e.g. [20]; $\langle n \rangle$ is the density; $k = (\mathbf{k}, \nu)$ and $q = (\mathbf{q}, \omega)$ denote fermionic and bosonic momentum-energy four-vectors, respectively, ν, ω are Matsubara frequencies. Summations over k, q imply a factor $T, \frac{1}{N}$ where T is the temperature and N the number of lattice sites. The *Hedin vertex* $\gamma^{\text{ch(sp)}}$ takes, in the exact theory, all vertex corrections in the particle-hole channel into account.

The screened interactions W corresponds to the bare Hubbard interaction $U^{\text{ch}} = U, U^{\text{sp}} = -U, U^{\text{s}} = 2U, U^{\text{t}} = 0$ in the charge (ch) and spin (sp), singlet (s), triplet (t) channel, respectively, dressed by the polarization Π , i.e.,

$$W_q^{\text{ch/sp}} = \frac{U^{\text{ch/sp}}}{1 - U^{\text{ch/sp}} \Pi_q^{\text{ch/sp}}}, \quad W_q^{\text{s}} = \frac{U^{\text{s}}}{1 - \frac{1}{2} U^{\text{s}} \Pi_q^{\text{s}}}. \quad (2)$$

For later use, we here introduced a W^{s} also for the singlet particle-particle channel, while $W^{\text{t}} = 0$. Both are not used in Hedin's original $GW\gamma$ approach, but are needed for the later connection to the parquet approach, which includes the particle-particle channel. The third, transversal particle-hole, channel is related to the particle-hole channel by crossing symmetry. Hence we do not need to introduce two further W 's and γ 's; $W^{\text{ch(sp)}}$ and $\gamma^{\text{ch(sp)}}$ in the particle-hole channel are sufficient.

The polarization in Eq. (2) is in turn given by the Hedin vertex:

$$\Pi_q^{\text{ch/sp}} = \sum_k G_k G_{k+q} \gamma_{kq}^{\text{ch/sp}}, \quad \Pi_q^{\text{s}} = \sum_k G_k G_{q-k} \gamma_{kq}^{\text{s}}. \quad (3)$$

Equations (1)-(3) are formally exact, but in general the vertex corrections contained in γ are unknown. Hedin [3] suggested to calculate these through the Ward identity (see also Sec. V) but this is hardly feasible in practice. Instead, the vertex corrections γ are often neglected which gives rise to the eponymous GW approximation. If (some approximate) vertex corrections are kept one speaks of a $GW\gamma$ approach [45].

The diagrammatic background to introduce W and Π in the Hedin equations is the concept of interaction-(ir)reducibility: a Feynman diagram is interaction-reducible if and only if it separates into two pieces if one interaction line is cut out. Eventually, we need to consider all vertex corrections, i.e., the full vertex function $F_{kk'q}^{\alpha}$. The interaction-reducible diagrams of F take the form [38],

$$\Delta_{kk'q}^{\alpha} = \gamma_{kq}^{\alpha} W_q^{\alpha} \gamma_{k'q}^{\alpha}. \quad (4)$$

Quite obviously, we can cut an interaction line U within W and hence Δ , and vice versa any interaction-reducible diagram in channel α has to be of the form Eq. (4). The vertex Δ has been coined *single-boson exchange* (SBE) vertex [38] as it involves the exchange of a single boson with four-vector q within W .

These interaction-reducible contributions must not be contained in γ , and hence must be subtracted from F to avoid a double counting [46]. This yields [38]:

$$\gamma_{kq}^{\text{ch/sp}} = 1 + \sum_{k'} (F_{kk'q}^{\text{ch/sp}} - \Delta_{kk'q}^{\text{ch/sp}}) G_{k'} G_{k'+q}, \quad (5a)$$

$$\gamma_{kq}^{\text{s}} = -1 + \frac{1}{2} \sum_{k'} (F_{kk'q}^{\text{s}} - \Delta_{kk'q}^{\text{s}}) G_{k'} G_{q-k'}. \quad (5b)$$

Here, the Green's functions serve the conversion of the four point vertex $F - \Delta$ to the three point vertex γ , and the "1" generates in the Hedin formulations the contributions without vertex corrections. There is no triplet Hedin vertex because the bare interaction vanishes in this channel, $U^{\text{t}} = 0$.

III. PARQUET FORMALISM

The parquet formalism [1, 2, 4, 20, 47] is based on the insight that the full vertex F can be decomposed into the fully-irreducible vertex Λ and reducible vertices Φ^r in the particle-hole ($r = ph$), transversal-particle-hole ($r = \overline{ph}$) and particle-particle-channel ($r = pp$). Now (two-particle) irreducibility is to be understood with respect to cutting two Green's function lines. Each Feynman diagram for F belongs to exactly one of these four classes, i.e., $F = \Lambda + \Phi^{ph} + \Phi^{\overline{ph}} + \Phi^{pp}$ [4, 20]. In terms of the spin combinations $\alpha = \text{ch, sp}$, we get with the momentum-convention for the particle-hole channel (cf. Fig. 1, left),

$$F_{kk'q}^{\alpha} = \Lambda_{kk'q}^{\alpha} + \Phi_{kk'q}^{ph, \alpha} \quad (6)$$

$$- \frac{1}{2} \Phi_{k, k+q, k'-k}^{ph, \text{ch}} - \frac{3 - 4\delta_{\alpha, \text{sp}}}{2} \Phi_{k, k+q, k'-k}^{ph, \text{sp}}$$

$$+ \frac{1 - 2\delta_{\alpha, \text{sp}}}{2} \Phi_{kk', k+k'+q}^{pp, \text{s}} + \frac{3 - 2\delta_{\alpha, \text{sp}}}{2} \Phi_{kk', k+k'+q}^{pp, \text{t}}.$$

Here, we have expressed $\Phi^{\overline{ph}}$ in terms of Φ^{ph} in the second line using the crossing relation [6], and properly translated the s and t components and momenta of the pp channel in the third line. The fully irreducible vertex Λ

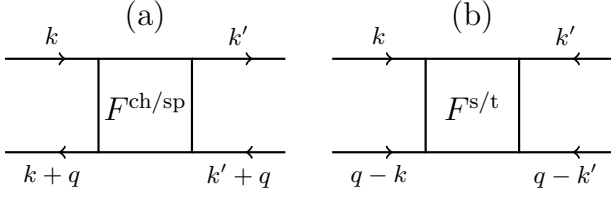


FIG. 1. Label convention for (a) the particle-hole and (b) the particle-particle notation.

or an approximation thereof, such as the *parquet approximation* $\Lambda^\alpha = U^\alpha$, serves as an input.

Since $\alpha = \text{ch, sp}$ and $\alpha = \text{s, t}$ already uniquely determine the channel $r = \text{ph}$ and $r = \text{pp}$, respectively, we drop the channel index r in the following.

There is only one F with two independent spin combinations, but one can use the singlet and triplet combinations and pp momentum convention (cf. Fig. 1), which is related to the above by

$$F_{kk'q}^{\text{s}} = \frac{1}{2} \left(F_{kk',q-k-k'}^{\text{ch}} - 3F_{kk',q-k-k'}^{\text{sp}} \right), \quad (7a)$$

$$F_{kk'q}^{\text{t}} = \frac{1}{2} \left(F_{kk',q-k-k'}^{\text{ch}} + F_{kk',q-k-k'}^{\text{sp}} \right). \quad (7b)$$

One can further introduce an irreducible vertex in the respective channel

$$\Gamma_{kk'q}^\alpha = F_{kk'q}^\alpha - \Phi_{kk'q}^\alpha. \quad (8)$$

For calculating the reducible vertices, we employ the Bethe-Salpeter equations which in terms of Φ read

$$\Phi_{kk'q}^{\text{ch/sp}} = \sum_{k''} \Gamma_{kk''q}^{\text{ch/sp}} G_{k''} G_{k''+q} F_{k''k'q}^{\text{ch/sp}}, \quad (9a)$$

$$\Phi_{kk'q}^{\text{s/t}} = \mp \frac{1}{2} \sum_{k''} \Gamma_{kk''q}^{\text{s/t}} G_{k''} G_{q-k''} F_{k''k'q}^{\text{s/t}}. \quad (9b)$$

Here, we can replace Γ by Eq. (8), which allows for a self-consistent calculation of Φ and F in the four-channels if Λ is known as an input. Further, G and Σ can be calculated self-consistently as well, using additionally the Dyson equation and Schwinger-Dyson equation [that is equivalent to Eq. (1)].

IV. A UNIFIED APPROACH TO VERTEX CORRECTIONS

We now relate the Hedin and parquet formalisms described in Sections II and III. Starting point is an analog to the parquet Eq. (6) but formulated in terms of interaction-(ir)reducible vertices instead of the two-particle (ir)reducibility of Eq. (6). This SBE decomposition [38] into interaction-reducible channels reads for

$\alpha = \text{ch, sp}$:

$$F_{kk'q}^\alpha = \Lambda_{kk'q}^{\text{Uirr},\alpha} + \Delta_{kk'q}^\alpha \quad (10)$$

$$- \frac{1}{2} \Delta_{k,k+q,k'-k}^{\text{ch}} - \frac{3-4\delta_{\alpha,\text{sp}}}{2} \Delta_{k,k+q,k'-k}^{\text{sp}}$$

$$+ \frac{1-2\delta_{\alpha,\text{sp}}}{2} \Delta_{kk',k+k'+q}^{\text{s}} - 2U^\alpha.$$

The essential difference to the parquet Eq. (6) is that the vertices Δ^α defined in Eq. (4) are reducible with respect to the bare interaction U^α [48]. The bare interaction is itself interaction-reducible and hence included in the Δ^α 's; thus we need to subtract $2U^\alpha$ in Eq. (10) to prevent an overcounting. As already discussed in Section II, $U^t = W^t = \Delta^t = 0$.

This also implies Λ^{Uirr} is fully irreducible with respect to the interaction, and must *not* be confused with the vertex Λ of the parquet decomposition Eq. (6) which is fully irreducible with respect to pairs of Green's functions. This implies on the one hand that U is contained in Λ but not in Λ^{Uirr} . But otherwise Λ contains fewer diagrams than Λ^{Uirr} as each diagram that is interaction reducible is also two-particle reducible since we can cut the two Green's functions on one side of the two-particle interaction instead of the interaction itself [49].

In the following we will relate the parquet equation (6) and the SBE generalization Eq. (10) of the Hedin formalism, and formulate a unified theory. To this end, we will pinpoint the difference between Λ^{Uirr} and Λ , which is denoted as [39] *multi-boson exchange* (MBE) diagrams M^α (the SBE diagrams Δ^α are not part of Λ^{Uirr} ; Fig. 3 below clarifies the multi-boson character of M). We will derive the equations to calculate M^α and Δ^α self-consistently in a unified Hedin and parquet formalism. This approach, while fully equivalent to the parquet approach, is formulated with the Hedin vertices and screened interactions and bears the advantage that the calculated vertex functions Λ^{Uirr}, M decay with the frequencies and depend only weakly on the momenta, compared to F, Φ of the original parquet approach.

First, we start with some definitions. Analogously to Γ^α in Eq. (8), we introduce vertices T^α that are irreducible with respect to the bare interaction U^α only in a particle-hole channel ($\alpha = \text{ch, sp}$) or in a particle-particle channel ($\alpha = \text{s, t}$) by removing the reducible diagrams Δ^α in that channel:

$$T_{kk'q}^\alpha = F_{kk'q}^\alpha - \Delta_{kk'q}^\alpha. \quad (11)$$

By comparison with Eqs. (5a) and (5b) we see that the vertices T describe the vertex corrections for the Hedin vertex γ . The latter is therefore also irreducible with respect to the bare interaction in the corresponding channel [38, 50].

As is the custom in Hedin's formalism we remove the bare interaction U^α from the irreducible vertex Γ^α :

$$S^\alpha = \Gamma^\alpha - U^\alpha. \quad (12)$$

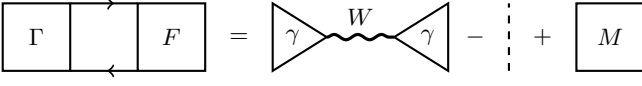


FIG. 2. Relation Eq. (14) between the particle-hole reducible vertices Φ in Eq. (9a) and M defined in Eq. (17a), which represents multi-boson exchange (cf. Fig. 3). Arrows and a dashed line denote Green's function G and the bare interaction U , respectively.

Now we collect all diagrams that are interaction-irreducible (but two-particle reducible) as the difference

$$M_{kk'q}^\alpha = T_{kk'q}^\alpha - S_{kk'q}^\alpha. \quad (13)$$

Conversely, this means that Φ^α consists of M^α plus the interaction-reducible vertices Δ^α in the respective channel,

$$\Phi_{kk'q}^\alpha = F_{kk'q}^\alpha - \Gamma_{kk'q}^\alpha = \Delta_{kk'q}^\alpha - U^\alpha + M_{kk'q}^\alpha. \quad (14)$$

Here again U^α needs to be subtracted as it is included in Δ^α but not in Φ^α . A diagrammatic representation of Eq. (14) is shown in Fig. 2 for the particle-hole channel. Note that $\Phi^t = M^t$ since $U^t = \Delta^t = 0$.

With these definitions, we can now relate $\Lambda^{\text{Uirr},\alpha}$ of the SBE decomposition Eq. (10) to Λ^α of the parquet Eq. (6), or more specifically to

$$\tilde{\Lambda}^\alpha = \Lambda^\alpha - U^\alpha. \quad (15)$$

To this end, we equate Eq. (10) to Eq. (6), which both yield F^α , and express Φ^α by M^α using Eq. (14). We are left with

$$\begin{aligned} \Lambda_{kk'q}^{\text{Uirr},\alpha} &= \tilde{\Lambda}_{kk'q}^\alpha + M_{kk'q}^\alpha \\ &= \frac{1}{2} M_{k,k+q,k'-k}^{\text{ch}} - \frac{3-4\delta_{\alpha,\text{sp}}}{2} M_{k,k+q,k'-k}^{\text{sp}} \\ &\quad + \frac{1-2\delta_{\alpha,\text{sp}}}{2} M_{kk',k+k'+q}^{\text{s}} + \frac{3-2\delta_{\alpha,\text{sp}}}{2} M_{kk',k+k'+q}^{\text{t}}. \end{aligned} \quad (16)$$

All Δ^α 's cancel, as it must be.

We still need to calculate the M^α 's. This can be done through Bethe-Salpeter-like equations similar as the Φ^α 's in Eq. (9) of the original parquet formalism. Starting with Eq. (9), substituting F^α , Γ^α and Φ^α by Eqs. (11), (12), and (14), respectively, and removing all interaction-reducible contributions from the left and right hand side, this yields

$$M_{kk'q}^{\text{ch/sp}} = \sum_{k''} S_{kk''q}^{\text{ch/sp}} G_{k''} G_{k''+q} T_{k''k'q}^{\text{ch/sp}}, \quad (17a)$$

$$M_{kk'q}^{\text{s/t}} = \mp \frac{1}{2} \sum_{k''} S_{kk''q}^{\text{s/t}} G_{k''} G_{q-k''} T_{k''k'q}^{\text{s/t}}. \quad (17b)$$

Here, $T = S + M$ [Eq.(13)] can be substituted.

Besides this Bethe-Salpeter equation, we need the eponymous parquet equation, i.e., Eq. (6) in the original parquet formalism. Moving Φ^α for the considered four channels (α) to the left hand side in Eq. (6) and reexpressing everything in terms of the new variables ($\Lambda^{\text{Uirr}}, M, \Delta$), we obtain, analogous to Ref. [39], the parquet equation formulated in terms of

$$S_{kk'q}^{\text{ch}} = \Lambda_{kk'q}^{\text{Uirr, ch}} - M_{kk'q}^{\text{ch}} - \frac{1}{2} \Delta_{k,k+q,k'-k}^{\text{ch}} - \frac{3}{2} \Delta_{k,k+q,k'-k}^{\text{sp}} + \frac{1}{2} \Delta_{kk',k+k'+q}^{\text{s}} - 2U^{\text{ch}}, \quad (18a)$$

$$S_{kk'q}^{\text{sp}} = \Lambda_{kk'q}^{\text{Uirr, sp}} - M_{kk'q}^{\text{sp}} - \frac{1}{2} \Delta_{k,k+q,k'-k}^{\text{ch}} + \frac{1}{2} \Delta_{k,k+q,k'-k}^{\text{sp}} - \frac{1}{2} \Delta_{kk',k+k'+q}^{\text{s}} - 2U^{\text{sp}}, \quad (18b)$$

$$S_{kk'q}^{\text{s}} = \Lambda_{kk'q}^{\text{Uirr, s}} - M_{kk'q}^{\text{s}} + \frac{1}{2} \Delta_{kk',q-k'-k}^{\text{ch}} - \frac{3}{2} \Delta_{kk',q-k'-k}^{\text{sp}} + \frac{1}{2} \Delta_{k,q-k',k'-k}^{\text{ch}} - \frac{3}{2} \Delta_{k,q-k',k'-k}^{\text{sp}} - U^{\text{ch}} + 3U^{\text{sp}}, \quad (18c)$$

$$S_{kk'q}^{\text{t}} = \Lambda_{kk'q}^{\text{Uirr, t}} - M_{kk'q}^{\text{t}} + \frac{1}{2} \Delta_{kk',q-k'-k}^{\text{ch}} + \frac{1}{2} \Delta_{kk',q-k'-k}^{\text{sp}} - \frac{1}{2} \Delta_{k,q-k',k'-k}^{\text{ch}} - \frac{1}{2} \Delta_{k,q-k',k'-k}^{\text{sp}}, \quad (18d)$$

which we need as input for the Bethe-Salpeter-like Eqs. (17a) and (17b).

The expressions for the ladder kernels S defined in Eqs. (18a)-(18d) elucidate the physical picture implied in the reformulated parquet equations: The parquet diagrams are reexpressed in terms of single- and multi-boson exchange, where the latter is represented by M which arises from the ladder Eq. (13) via repeated exchange of bosons, starting from the second order. The feedback of M on the ladder kernel S leads to the channel mixing that is characteristic of the parquet approach. Feynman dia-

grams corresponding to multi-boson exchange are shown in Fig. 3.

V. CALCULATION SCHEME

Now we are in a position to formulate a new *efficient* calculation scheme, called a *Boson Exchange Parquet Solver* (BEPS), which was introduced for dual fermions in Ref. [39]. The algorithm is as follows (for clarity, we repeat the most relevant equations):

Step 0 (starting point): Choose an approximation for $\tilde{\Lambda}$ (parquet approximation: $\tilde{\Lambda} \equiv 0$; DΓA: $\tilde{\Lambda} = \text{local}$). Make an initial guess for the self-energy Σ , polarization Π , Hedin vertices γ , and the MBE vertices M .

Step 1: Update the propagators (Green's function and screened interaction)

$$G_k = \frac{G_k^0}{1 - G_k^0 \Sigma_k}, \quad (19)$$

$$W_q^{\text{ch/sp}} = \frac{U^{\text{ch/sp}}}{1 - U^{\text{ch/sp}} \Pi_q^{\text{ch/sp}}}, \quad (20a)$$

$$W_q^{\text{s}} = \frac{U^{\text{s}}}{1 - \frac{1}{2} U^{\text{s}} \Pi_q^{\text{s}}}, \quad (20b)$$

where G^0 is the non-interacting Green's function.

Step 2: Obtain the interaction-reducible vertex

$$\Delta_{kk'q}^\alpha = \gamma_{kq}^\alpha W_q^\alpha \gamma_{k'q}^\alpha. \quad (21)$$

Step 3: Calculate the irreducible kernel S from Eqs. (18a)-(18d), where Λ^{Uirr} is obtained from M and the fixed $\tilde{\Lambda}$ through Eq. (16).

Step 4: With this S solve the ladder equations

$$M_{kk'q}^{\text{ch/sp}} = \sum_{k''} S_{kk''q}^{\text{ch/sp}} G_{k''} G_{k'+q} T_{k''k'q}^{\text{ch/sp}}, \quad (22a)$$

$$M_{kk'q}^{\text{s/t}} = \mp \frac{1}{2} \sum_{k''} S_{kk''q}^{\text{s/t}} G_{k''} G_{q-k''} T_{k''k'q}^{\text{s/t}}, \quad (22b)$$

using $T_{kk'q}^\alpha = S_{kk'q}^\alpha + M_{kk'q}^\alpha$.

Step 5: Update the Hedin vertices

$$\gamma_{kq}^{\text{ch/sp}} = 1 + \sum_{k'} (F_{kk'q}^{\text{ch/sp}} - \Delta_{kk'q}^{\text{ch/sp}}) G_{k'} G_{k'+q}, \quad (23a)$$

$$\gamma_{kq}^{\text{s}} = -1 + \frac{1}{2} \sum_{k'} (F_{kk'q}^{\text{s}} - \Delta_{kk'q}^{\text{s}}) G_{k'} G_{q-k'}. \quad (23b)$$

Here, F is expressed through the SBE decomposition Eq. (10) and the parquet expression Eq. (16).

Step 6: Update the self-energy and polarization

$$\Sigma_k = \frac{U\langle n \rangle}{2} - \frac{1}{2} \sum_q G_{k+q} \left[W_q^{\text{ch}} \gamma_{kq}^{\text{ch}} + W_q^{\text{sp}} \gamma_{kq}^{\text{sp}} \right], \quad (24)$$

$$\Pi_q^{\text{ch/sp}} = \sum_k G_k G_{k+q} \gamma_{kq}^{\text{ch/sp}}, \quad (25a)$$

$$\Pi_q^{\text{s}} = \sum_k G_k G_{q-k} \gamma_{kq}^{\text{s}}. \quad (25b)$$

Iterate steps 1 to 6 until convergence.

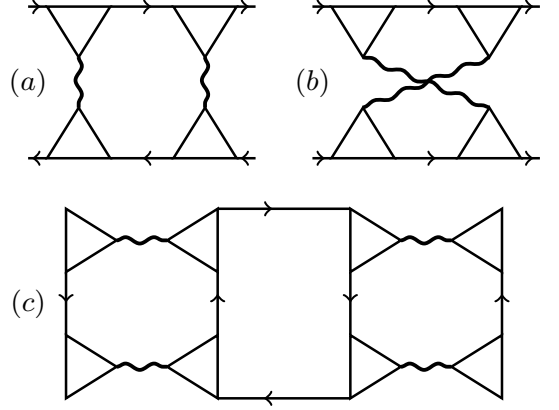


FIG. 3. Exemplary vertex corrections corresponding to multiple boson exchange, see also Ref. [39]. Diagrams (a) and (b) represent boson exchange in the particle-hole (a) and particle-particle (b) channels. Diagram (c) corresponds to a mixing of horizontal and vertical particle-hole channels.

In Step 3 the ladder kernel S is calculated *on-the-fly* for only one bosonic momentum-energy q at a time. In Step 4 the vertices T need not be evaluated, only M are stored. As a result, the Hedin vertices in Eqs. (23a) and (23b) can be expressed in terms of $\tilde{\Lambda}$, Δ , and M . Only the quantities mentioned in Step 0 need to be stored and updated over the iterations.

Relation to Hedin's equations: The calculation scheme above differs from Hedin's original work through the prescription for the ladder kernel S in Step 3. In Hedin's equations [16, 17] the ladder kernel is given by the functional derivative $S = \delta(\Sigma - \Sigma^H) / \delta G$ where $\Sigma^H = U\langle n \rangle / 2$. With this S and using $F - \Delta = T$ in Eq. (23a) the algorithm is equivalent to Hedin's equations. This functional derivative is however difficult to calculate in practice. Here, instead, S is obtained from the parquet diagrams in Step 3, as proved in Sec. IV.

VI. APPLICATIONS

A. Atomic Limit

We apply the BEPS method to a toy model, the atomic limit of e.g. the Hubbard model at half-filling. This model is exactly solvable and it has a nontrivial solution for the vertex functions. Analytical expressions for all components of the parquet decomposition Eq. (6) are available [51]. Starting from the exact fully irreducible vertex $\Lambda_{\nu\nu'\omega}$ the calculation cycle in Sec. V recovers the correlation functions of the atomic limit.

A Python implementation [42] is provided which converges on a single core within a few minutes [52].

We focus here on one advantage of the BEPS calculation scheme, evident already in the atomic limit, which

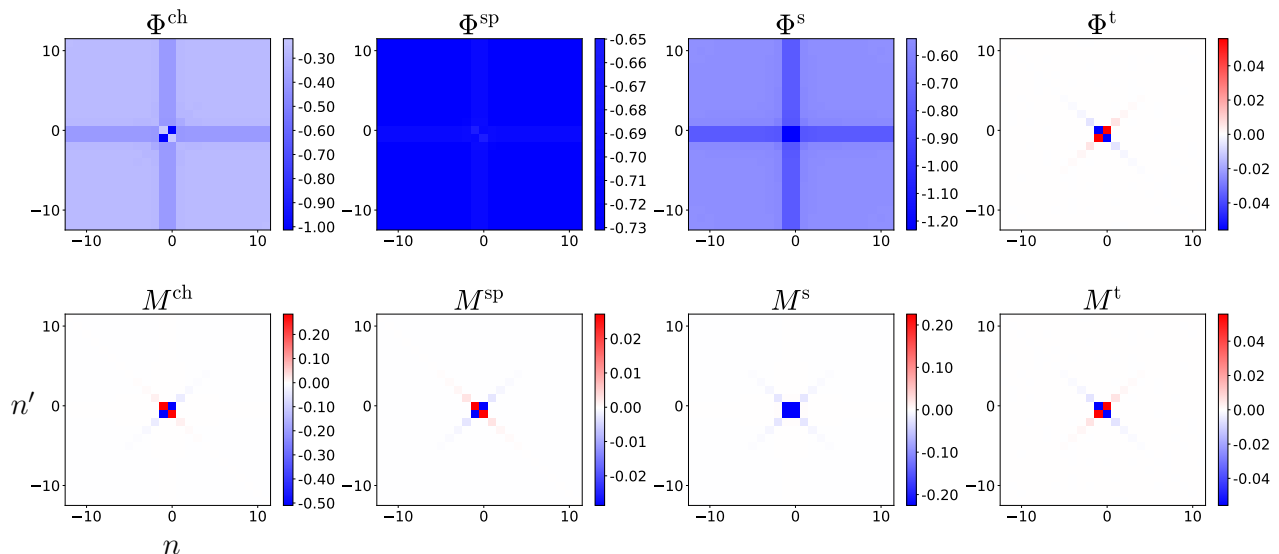


FIG. 4. Reducible vertex functions of the atomic limit at $U/T = 2$. Axes show the fermionic Matsubara indices ($\omega = 0$). Top: Φ corresponding to the original parquet decomposition Eq. (6). Bottom: Vertices M of the parquet expression Eq. (16).

is the decay of the vertex functions at high frequencies. The top panels of Fig. 4 show the reducible vertices $\Phi_{\nu\nu'\omega}$ of the parquet decomposition in Eq. (6). The vertices belonging to the channels $\alpha = \text{ch, sp, s}$ have features that do not decay at high frequencies, whereas the triplet vertex $\alpha = \text{t}$ decays. This is the case because the bare interaction vanishes in the triplet channel, $U^t = 0$. The bottom panels of Fig. 4 show the corresponding vertices $M_{\nu\nu'\omega}$ of the parquet expression (16). Evidently, all features of these vertices decay at high frequency (in case of the triplet channel trivially because $M^t = \Phi^t$).

B. Parquet approximation

Next, we analyze the vertices in the parquet approximation for the weakly interacting Hubbard model on the square lattice at half-filling, $U/t = 2$, where $t = 1$ is the nearest neighbor hopping amplitude. The temperature is set to $T/t = 0.2$. The lattice size is fixed to 8×8 sites.

The *victory* implementation of the parquet method which we use here was presented in Ref. [9]. It does not make use of the efficient calculation scheme presented in Sec. V, but it serves us to evaluate the vertices F and Φ within the parquet approximation.

As mentioned above, in the efficient calculation scheme the parquet approximation corresponds to setting the fully irreducible vertex in Eq. (16) to zero, $\hat{\Lambda}^\alpha = 0$, whereas the *victory* implementation actually evaluates Eq. (6) using $\Lambda^\alpha = \hat{\Lambda}^\alpha + U^\alpha = U^\alpha$. We show in Appendix A how the vertices M can be calculated from the converged solution for F and Φ . Their full momentum and frequency dependence is available to us,

$$M^{\text{ch/sp}}(\mathbf{k}, \mathbf{k}', \mathbf{q}, \nu, \nu', \omega). \quad (26)$$

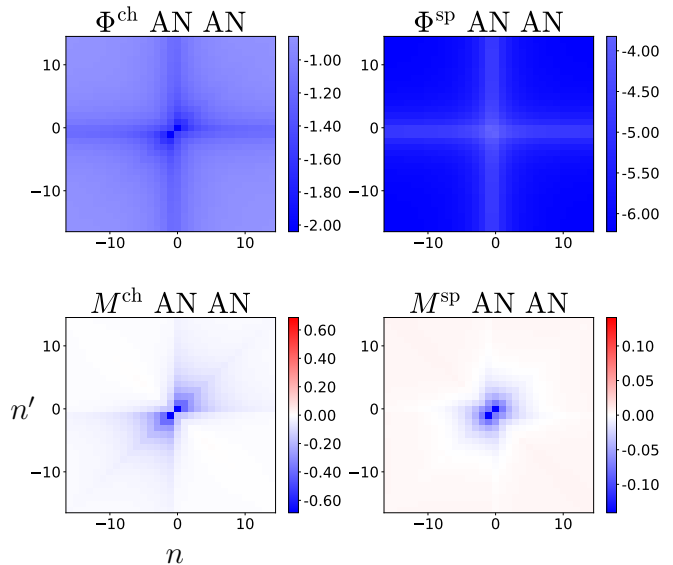


FIG. 5. Reducible vertex functions in the parquet approximation, $U/t = 2, T/t = 0.2$. Fermionic momenta correspond to the antinode (AN), $\mathbf{q} = (\pi, \pi)$, other labels as in Fig. 4.

First, we consider the asymptotic behavior of the vertices as a function of the frequencies. Fig. 5 shows the particle-hole vertices $\Phi^{\text{ch/sp}}$ and $M^{\text{ch/sp}}$, where we focus on the antinode, $\mathbf{k} = \mathbf{k}' = \mathbf{k}_{\text{AN}} = (\pi, 0)$, the bosonic momentum and frequency are set to $\mathbf{q} = (\pi, \pi)$ and $\omega = 0$. This combination represents the scattering of particle and hole from the antinode to another antinode.

Similar to the atomic limit, the M 's decay as a function of ν, ν' in all directions, but their structure is more complicated due to the additional energy scale t .

We note that in the current implementation it is not

VII. CONCLUSIONS

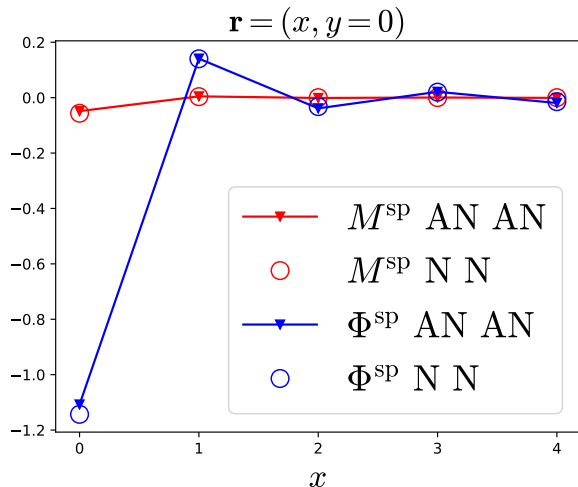


FIG. 6. Spatial dependence of Φ^{SP} and M^{SP} . The fermionic momenta correspond to the node or antinode. The alternating sign of Φ^{SP} indicates antiferromagnetic correlations.

feasible to fully converge the Matsubara summations required for the calculation of the vertices M (cf. Appendix A). The correspondence to the calculated Φ is therefore not perfect and M^{SP} retains a small residual asymptote.

Next, we consider the spatial dependence of the vertices. To this end, we transform Φ^{SP} and M^{SP} to real space with respect to the bosonic momentum, $\mathbf{q} \rightarrow \mathbf{r}$,

$$M^{\text{ch/sp}}(\mathbf{k}, \mathbf{k}', \mathbf{r}, \nu, \nu', \omega). \quad (27)$$

We fix the frequencies to $\nu = \nu' = \pi T$, $\omega = 0$. For the fermionic momenta we consider the antinode $\mathbf{k} = \mathbf{k}' = \mathbf{k}_{\text{AN}}$ and the node $\mathbf{k} = \mathbf{k}' = \mathbf{k}_{\text{N}} = (\frac{\pi}{2}, \frac{\pi}{2})$.

Fig. 6 shows Φ^{SP} and M^{SP} as a function of $\mathbf{r} = (x, y = 0)$ along the x -axis. Clearly visible is the alternating sign of Φ^{SP} characteristic of antiferromagnetic correlations. On the other hand, M^{SP} is two orders of magnitude smaller than Φ^{SP} . Similarly, in the charge channel M^{ch} is much smaller than Φ^{ch} (not shown). Importantly, this fact alone implies that the spatial dependence of $\Phi = M + \Delta - U$ is largely determined by Δ , the single-boson exchange [39]. It explains the fast convergence of the truncated unity approximation [53] used in Ref. [39], where only the M 's were truncated in real space while the full spatial dependence of Δ was retained.

Nonetheless, as mentioned above, the M^{SP} presented here was obtained in postprocessing and is not perfectly converged. Therefore, it may be the case that some residual antiferromagnetic correlations correspond to this vertex. In the future, the implementation of the efficient calculation scheme presented in Sec. V may ultimately clarify this, because it allows determining M with the same accuracy as Φ .

The parquet equations for real fermions were reformulated into a computationally more feasible form by combining them with Hedin's $GW\gamma$ formalism. From the viewpoint of the latter our approach yields the parquet diagrams for γ in terms of single- and multi-boson exchange. This offers a new perspective on vertex corrections in electronic systems. For example, the association of certain vertex diagrams with effective particles becomes very explicit [54], or the notion of a 'bosonic glue' that may play a role for phenomena such as high temperature superconductivity [55] can be taken more literally.

The resulting calculation scheme, which was coined a boson exchange parquet solver (BEPS) in Ref. [39], has no disadvantages in comparison to previous implementations of the parquet equations but offers two strong advantages. Namely, the vertex asymptotics and, in the case of a lattice system [39], also the long-ranged fluctuations are removed from the parquet equations through their exact reformulation.

This goes beyond the asymptotic treatment of the vertices pioneered in Refs. [8, 43, 56] which improves the feasibility of parquet solvers [8, 57, 58], but the low-energy aspect of the single-boson exchange remains intermixed with all other fluctuations. Instead, the BEPS method corresponds to a kind of separation of the fluctuations that is exact also at low frequencies [59, 60]. In Ref. [39] and here this idea was adopted to the parquet formalism for dual fermions and real fermions, respectively.

In the applications we first discussed the simple case of a quantum impurity model, where the spatial degrees of freedom do not play a role. The computational efficiency of the calculation scheme is then improved only by the decay properties of the vertices. Remarkably, this is sufficient to solve the parquet equations for the atomic limit on a laptop using the provided Python script [42].

We also analyzed the parquet approximation for the lattice Hubbard model using the *victory* code presented in Ref. [9]. We evaluated the vertices that correspond to the BEPS method and verified that they indeed exhibit the useful decay properties. This underlines the accuracy of the asymptotic treatment of the vertices in this implementation [8].

In the future we will however implement the efficient calculation scheme into the *victory* code [9]. This seems promising because in Ref. [39], which discussed the lattice case for dual fermions, it is shown that the BEPS method unfolds its full power in combination with the truncated unity (TU) approximation [53, 61–64], which corresponds to a real space truncation of the vertices. We expect also for real fermions a similar improved convergence with the form factors compared to the truncated unity parquet solver (TUPS, [53]). While the form factors correspond to a suitable basis for the spatial degrees of freedom, the computational efficiency may be further improved by introducing an optimal basis for the frequencies [65].

Lastly, some words are in place regarding the closely related method for dual fermions presented in Ref. [39]: Diagrammatically, both approaches are the same, but the basic building blocks are different. In Ref. [39] the (real fermion) Green's function lines are replaced by dual fermion lines and the equations defining the self-energy, polarization, and Hedin vertex assume a different form. In the present paper, the starting point is an approximation for the two-particle fully irreducible vertex Λ . In contrast, in the dual fermion formulation [39] local *reducible* interactions are included, hence using, e.g., a local full vertex F_{loc} for dual fermions instead of a local Λ_{loc} in DfA. This leads to an interesting distinction between the bosonization of the parquet equations for real and dual fermions, respectively, which corresponds to removing the interaction-reducible diagrams from either F_{loc} or Λ_{loc} : In case of lattice fermions Λ_{loc} includes only one such diagram, the bare interaction itself, whereas for dual fermions F_{loc} contains many interaction-reducible diagrams which need to be separated off using the (local) SBE decomposition [38].

The approaches for real and lattice fermions both have their pros and cons. The parquet solver discussed in the present paper is simpler, an integral part of many different approaches, the interpretation in terms of real fermions is easier, and the approximation made for Λ is very explicit. On the other hand, the connecting dual fermion lines decay much faster, which, in combination with the decay of the vertex functions facilitated by the BEPS method, leads to a very high computational efficiency of the dual parquet solver [39]. Further, the dual fermions are not affected by divergences of the vertex Λ_{loc} [66].

ACKNOWLEDGMENTS

We thank C. Eckhardt, A. Valli, and M. Wallerberger for useful comments on the text and S. Andergassen, M. Capone, P. Chalupa, C. Hille, M. Kitatani, A.I. Lichtenstein, E.G.C.P. van Loon, G. Rohringer, and A. Toschi for discussions. The present research was supported by the Austrian Science Fund (FWF) through projects P32044 and P30997.

Appendix A: Evaluation of vertices M

Here, we show how the vertices M^α in the parquet expression (16) can be calculated from a converged result of the *victory* code [9], that is, the Green's function G and the vertices Φ and F in the parquet decomposition (6) are known. We focus on the particle-hole channels $\alpha = \text{ch, sp}$.

First, we determine the susceptibility and the screened interaction,

$$\begin{aligned} X_q^\alpha &= 2 \sum_k G_k G_{k+q} + 2 \sum_{kk'q} G_k G_{k+q} F_{kk'q}^\alpha G_{k'} G_{k'+q}, \\ W_q^\alpha &= U^\alpha \left(1 + \frac{1}{2} X_q^\alpha U^\alpha \right). \end{aligned} \quad (\text{A1})$$

Next, we evaluate the Hedin vertex γ . We insert Eq. (4) into Eq. (5a),

$$\begin{aligned} \gamma_{kq}^\alpha &= 1 + \sum_{k'} (F_{kk'q}^\alpha - \gamma_{kq}^\alpha W_q^\alpha \gamma_{k'q}^\alpha) G_{k'} G_{k'+q} \\ &= 1 + \sum_{k'} F_{kk'q}^\alpha G_{k'} G_{k'+q} - \gamma_{kq}^\alpha W_q^\alpha \Pi_q^\alpha \\ &= 1 + \sum_{k'} F_{kk'q}^\alpha G_{k'} G_{k'+q} - \gamma_{kq}^\alpha \frac{1}{2} U^\alpha X_q^\alpha. \end{aligned} \quad (\text{A2})$$

From the first to the second line we identified the polarization Π using Eq. (3). From the second to the third line we used Eq. (2) and $X_q^\alpha = 2\Pi_q^\alpha / (1 - U^\alpha \Pi_q^\alpha)$. We solve Eq. (A2) for γ ,

$$\gamma_{kq}^\alpha = \frac{1 + \sum_{k'} F_{kk'q}^\alpha G_{k'} G_{k'+q}}{W_q^\alpha / U^\alpha}, \quad (\text{A3})$$

where we used again Eq. (A1). With γ and W we finally obtain M from Eq. (14) (see also Fig. 2),

$$M_{kk'q}^\alpha = \Phi_{kk'q}^\alpha - \gamma_{kq}^\alpha W_q^\alpha \gamma_{k'q}^\alpha + U^\alpha. \quad (\text{A4})$$

We do not evaluate $M^{s/t}$ in the particle-particle channel. However, for the singlet channel $\alpha = s$ the steps are analogous, starting from Eq. (5b) and taking into account the factor $\frac{1}{2}$. For the triplet channel nothing needs to be done since $M^t = \Phi^t$.

-
- [1] C. De Dominicis and P. C. Martin, *Journal of Mathematical Physics* **5**, 14 (1964).
 - [2] C. De Dominicis and P. C. Martin, *Journal of Mathematical Physics* **5**, 31 (1964).
 - [3] L. Hedin, *Phys. Rev.* **139**, A796 (1965).
 - [4] N. E. Bickers, "Self-consistent many-body theory for condensed matter systems," in *Theoretical Methods for Strongly Correlated Electrons*, edited by D. Sénéchal, A.-M. Tremblay, and C. Bourbonnais (Springer New York, New York, NY, 2004) pp. 237–296.
 - [5] K.-M. Tam, H. Fotsos, S.-X. Yang, T.-W. Lee, J. Moreno, J. Ramanujam, and M. Jarrell, *Phys. Rev. E* **87**, 013311 (2013).
 - [6] G. Rohringer, A. Valli, and A. Toschi, *Phys. Rev. B* **86**, 125114 (2012).
 - [7] A. Valli, T. Schäfer, P. Thunström, G. Rohringer, S. Andergassen, G. Sangiovanni, K. Held, and A. Toschi, *Phys. Rev. B* **91**, 115115 (2015).
 - [8] G. Li, N. Wentzell, P. Pudleiner, P. Thunström, and K. Held, *Phys. Rev. B* **93**, 165103 (2016).

- [9] G. Li, A. Kauch, P. Pudleiner, and K. Held, *Comput. Phys. Commun.* **241**, 146 (2019).
- [10] G. V. Astretsov, G. Rohringer, and A. N. Rubtsov, *Phys. Rev. B* **101**, 075109 (2020).
- [11] S. Friederich, H. C. Krahl, and C. Wetterich, *Phys. Rev. B* **83**, 155125 (2011).
- [12] W. Metzner, M. Salmhofer, C. Honerkamp, V. Meden, and K. Schönhammer, *Rev. Mod. Phys.* **84**, 299 (2012).
- [13] A. Tagliavini, C. Hille, F. B. Kugler, S. Andergassen, A. Toschi, and C. Honerkamp, *SciPost Phys.* **6**, 9 (2019).
- [14] A. Kauch, F. Hörbinger, G. Li, and K. Held, “Interplay between magnetic and superconducting fluctuations in the doped 2d hubbard model,” (2019), [arXiv:1901.09743](https://arxiv.org/abs/1901.09743).
- [15] P. Pudleiner, A. Kauch, K. Held, and G. Li, *Phys. Rev. B* **100**, 075108 (2019).
- [16] G. Onida, L. Reining, and A. Rubio, *Rev. Mod. Phys.* **74**, 601 (2002).
- [17] K. Held, C. Taranto, G. Rohringer, and A. Toschi, “Hedin equations, gw, gw+dmft, and all that,” (2011), [arXiv:1109.3972](https://arxiv.org/abs/1109.3972).
- [18] A. Toschi, A. A. Katanin, and K. Held, *Phys. Rev. B* **75**, 045118 (2007).
- [19] A. A. Katanin, A. Toschi, and K. Held, *Phys. Rev. B* **80**, 075104 (2009).
- [20] G. Rohringer, H. Hafermann, A. Toschi, A. A. Katanin, A. E. Antipov, M. I. Katsnelson, A. I. Lichtenstein, A. N. Rubtsov, and K. Held, *Rev. Mod. Phys.* **90**, 025003 (2018).
- [21] R. W. Godby, M. Schlüter, and L. J. Sham, *Phys. Rev. B* **37**, 10159 (1988).
- [22] F. Aryasetiawan and O. Gunnarsson, *Reports on Progress in Physics* **61**, 237 (1998).
- [23] S. Biermann, F. Aryasetiawan, and A. Georges, *Phys. Rev. Lett.* **90**, 086402 (2003).
- [24] J. M. Tomczak, P. Liu, A. Toschi, G. Kresse, and K. Held, *The European Physical Journal Special Topics* **226**, 2565 (2017).
- [25] F. Nilsson, L. Boehnke, P. Werner, and F. Aryasetiawan, *Phys. Rev. Materials* **1**, 043803 (2017).
- [26] E. Maggio and G. Kresse, *J. Chem. Theory Comput.* **13**, 4765 (2017).
- [27] R. A. Smith, *Phys. Rev. A* **46**, 4586 (1992).
- [28] V. Janiš, *Phys. Rev. B* **60**, 11345 (1999).
- [29] V. Janiš and J. Kolorenč, *Phys. Rev. B* **71**, 245106 (2005).
- [30] V. Janiš, A. Kauch, and V. Pokorný, *Phys. Rev. B* **95**, 045108 (2017).
- [31] F. B. Kugler and J. von Delft, *New Journal of Physics* **20**, 123029 (2018).
- [32] F. Krien, *Conserving dynamical mean-field approaches to strongly correlated systems*, PhD Thesis (Hamburg, 2018).
- [33] C.-O. Almbladh, U. von Barth, and R. van Leeuwen, *International Journal of Modern Physics B* **13**, 535 (1999).
- [34] A. V. Chubukov and P. Wölfle, *Phys. Rev. B* **89**, 045108 (2014).
- [35] A. I. Larkin and A. A. Varlamov, in *Superconductivity* (Springer Berlin Heidelberg) pp. 369–458.
- [36] L. Aslamasov and A. Larkin, *Physics Letters A* **26**, 238 (1968).
- [37] D. Bergeron, V. Hankevych, B. Kyung, and A.-M. S. Tremblay, *Phys. Rev. B* **84**, 085128 (2011).
- [38] F. Krien, A. Valli, and M. Capone, *Phys. Rev. B* **100**, 155149 (2019).
- [39] F. Krien, A. Valli, P. Chalupa, M. Capone, A. I. Lichtenstein, and A. Toschi, “Boson exchange parquet solver (for dual fermions),” (2020), [arXiv:2008.04184](https://arxiv.org/abs/2008.04184).
- [40] A. N. Rubtsov, M. I. Katsnelson, and A. I. Lichtenstein, *Phys. Rev. B* **77**, 033101 (2008).
- [41] In the preprint of Ref. [39] it is stated in the conclusions that a boson exchange parquet solver can probably not be constructed for lattice fermions. This speculation is not correct, as is shown in this work. The statement will be corrected in the published version of Ref. [39].
- [42] F. Krien, “Boson exchange parquet solver,” <https://github.com/fkrien/beps> (2020).
- [43] N. Wentzell, G. Li, A. Tagliavini, C. Taranto, G. Rohringer, K. Held, A. Toschi, and S. Andergassen, *Phys. Rev. B* **102**, 085106 (2020).
- [44] We use a Fierz splitting of $\frac{1}{2}$ between charge and spin channels [67].
- [45] R. Del Sole, L. Reining, and R. W. Godby, *Phys. Rev. B* **49**, 8024 (1994).
- [46] Due to this *interaction-irreducible* property of the Hedin vertex it satisfies the ladder equations [3],
- $$\gamma_{kq}^{\text{ch/sp}} = 1 + \sum_{k'} S_{kk'q}^{\text{ch/sp}} G_{k'} G_{k'+q} \gamma_{k'q}^{\text{ch/sp}},$$
- $$\gamma_{kq}^{\text{s}} = -1 - \frac{1}{2} \sum_{k'} S_{kk'q}^{\text{s}} G_{k'} G_{q-k'} \gamma_{k'q}^{\text{s}},$$
- where S is the corresponding Bethe-Salpeter kernel *without* the bare interaction, defined in Eq. (12).
- [47] O. Gunnarsson, T. Schäfer, J. P. F. LeBlanc, J. Merino, G. Sangiovanni, G. Rohringer, and A. Toschi, *Phys. Rev. B* **93**, 245102 (2016).
- [48] One may also say that the vertices $\Delta = \gamma W \gamma$ are reducible with respect to the screened interaction W , however, it is useful to consider also the bare interaction diagram U as *reducible* [38]. Interestingly, the bare interaction does not play a role after we have passed over to the parquet expression Eq. (16), which implies that W -reducibility is a meaningful concept *after* the bosonization. Indeed, in a functional formulation of the GW approach the screened interaction plays the role of a fundamental variable [33].
- [49] Compare also Figs. 3 and 4 in Ref. [38]. In other words, interaction reducibility *implies* two-particle reducibility, with the only exception of the bare interaction itself, which is (fully) two-particle irreducible.
- [50] G. Rohringer and A. Toschi, *Phys. Rev. B* **94**, 125144 (2016).
- [51] P. Thunström, O. Gunnarsson, S. Ciuchi, and G. Rohringer, *Phys. Rev. B* **98**, 235107 (2018).
- [52] Due to the exponential difference between charge and spin fluctuations in the atomic limit the linear mixing used in the provided script does not work for large values of U/T . A nonlinear root-finder improves the convergence [67].
- [53] C. J. Eckhardt, C. Honerkamp, K. Held, and A. Kauch, *Phys. Rev. B* **101**, 155104 (2020).
- [54] A. Kauch, P. Pudleiner, K. Astleithner, P. Thunström, T. Ribic, and K. Held, *Phys. Rev. Lett.* **124**, 047401 (2020).
- [55] M. Kitatani, T. Schäfer, H. Aoki, and K. Held, *Phys. Rev. B* **99**, 041115 (2019).
- [56] J. Kuneš, *Phys. Rev. B* **83**, 085102 (2011).
- [57] A. Tagliavini, S. Hummel, N. Wentzell, S. Andergassen,

- A. Toschi, and G. Rohringer, *Phys. Rev. B* **97**, 235140 (2018).
- [58] J. Kaufmann, *Calculation of Vertex Asymptotics from Local Correlation Functions*, Master Thesis, TU Wien (2017).
- [59] F. Krien, *Phys. Rev. B* **99**, 235106 (2019).
- [60] A. Katanin, *Phys. Rev. B* **101**, 035110 (2020).
- [61] C. Husemann and M. Salmhofer, *Phys. Rev. B* **79**, 195125 (2009).
- [62] X. Wang, M. J. Han, L. de' Medici, H. Park, C. A. Marianetti, and A. J. Millis, *Phys. Rev. B* **86**, 195136 (2012).
- [63] C. Platt, W. Hanke, and R. Thomale, *Advances in Physics* **62**, 453 (2013), <https://doi.org/10.1080/00018732.2013.862020>.
- [64] J. Lichtenstein, D. Snchez de la Pea, D. Rohe, E. Di Napoli, C. Honerkamp, and S. Maier, *Computer Physics Communications* **213**, 100 (2017).
- [65] H. Shinaoka, J. Otsuki, K. Haule, M. Wallerberger, E. Gull, K. Yoshimi, and M. Ohzeki, *Phys. Rev. B* **97**, 205111 (2018).
- [66] T. Schäfer, G. Rohringer, O. Gunnarsson, S. Ciuchi, G. Sangiovanni, and A. Toschi, *Phys. Rev. Lett.* **110**, 246405 (2013).
- [67] F. Krien and A. Valli, *Phys. Rev. B* **100**, 245147 (2019).